The Connection between real-ω and real-k Approaches in an Absorbing Medium

Mehmet Emre Taşgın

***Abstract*—We investigate the transmission and reflection of a pulse that is incident from air on to an absorbing medium of frequency dependent dielectric. In the literature solution on the absorbing part is expressed as the fourier integral over all real frequency (ω) range, with corresponding complex wave-vectors $k = k_R(\omega) + ik_I(\omega)$. We show that, the solution in the absorbing part must be written as the Fourier sum of all real wave-vectors (k), with the corresponding complex frequencies $\omega = \omega_R(k) + i\omega_I(k)$. Then, we try to show that these two approaches result in different function, in space and time, for the transmitted pulse. On the contrary, we show that two approaches give the same result.**

On the other hand, we manage to derive a mathematical connection between the fourier components of the two approaches. This makes the comparison of the two types of group velocities accessible; with fixed position and with fixed time. We calculate a velocity in two different ways: using the i) real-ω and ii) real-k approaches. Then we compare the two results and decide if the velocity definition is reliable or not. This paper is the complementary work leading to Ref. [1]

***Index Terms*—group velocity, dispersive medium, superluminal propagation, real frequency, complex frequency, pulse reshape.**

I. Introduction

We consider the problem of pulse transmission from air to an absorbing medium of complex dielectric susceptibility $\epsilon(\omega) = \epsilon_R(\omega) + i\epsilon_R(\omega)$ which gives a complex index $n(\omega) = n_R(\omega) + in_I(\omega)$.

The solution of the Maxwell equations in complex indexed medium is given, [2], [3], by the integral sum of the real frequency fourier components such as

$$E(x,t) = \int_{-\infty}^{\infty} d\omega e^{-i\omega t} \quad \Big(C_1(\omega)e^{in(\omega)\omega x/c} + D_1(\omega)e^{-in(\omega)\omega x/c}\Big). \quad (1)$$

In section II-A we show that, in the general solution of the Maxwell equations in complex indexed medium, wave-vector k must be treated real. Treating k as a real variable brings out the complexity of the frequency ω. Furthermore, according to the usual model of absorption, as well as the polarization, this phenomenon is a behavior due to the time response of the atoms. This brings out the decision that the solutions must decay in time, locally.

M.E. Tasgin is with the Department of Electrical & Electronics Engineering, Kırklareli University, Kırklareli, Karahıdır 39020 Turkey and Center for Advanced Research, Kırklareli University, Kırklareli, Karahıdır 39020 Turkey e-mail: metasgin@kirklareli.edu.tr.

In contrast to the literature solution (1), we show that the general solution must be in the form of

$$E(x,t) = \int_{-\infty}^{\infty} dk e^{ikx} \left(C_2(k)e^{i\frac{ck}{n(k)}t} + D_2(k)e^{-i\frac{ck}{n(k)}t}\right), \quad (2)$$

where $n(k)$ is the index as a function of the real wave-vector k, treated in section II-B.

After then, we try to show the difference in between the two approach; real-ω approach and real-k approach. We use the boundary conditions(BC) in order to establish a connection between the fourier components of the two approaches in section III. The suspicion of the inequality of two approaches originates from the following decision. The equality of the sum of the fourier components at the boundary

$$\int_{-\infty}^{\infty} d\omega D_1(\omega)e^{-i\omega t} = \int_{-\infty}^{\infty} dk D_2(k)e^{-i\frac{ck}{n(k)}t} \quad (3)$$

does not imply the equality of the electric fields

$$\int_{-\infty}^{\infty} d\omega D_1(\omega)e^{i\omega n(\omega)x/c}e^{-i\omega t} = \int_{-\infty}^{\infty} dk D_2(k)e^{ikx}e^{-i\frac{ck}{n(k)}t} \quad (4)$$

in whole space and time. Carrying the integration over complex ω space may change the result of the two integrals in (4), due to the enclosed poles or branch cuts of $D_1(\omega)$, $D_2(k)$ or $n(k)$.

In section IV we try to show the difference of two approaches. For the cases, we considered here, there occurs no difference between results of the two approaches. However, we limited the behaviors of the functions such as the index $n(\omega)$ and the frequency distribution of the incident pulse $A(\omega)$. In example we limited $A(\omega)$ to convergent to zero at all infinities in the whole complex plane. This excludes the Gaussian functions, in example. Furthermore, in some dielectric mediums, created using three level systems, index $n(\omega)$ may exhibit strange behaviors, out of the lorentzian type.

So that, there exists the possibility of the presence of deviation from the equivalence of the two approaches for other types of incident pulse shapes.

Beyond the discussion of the equivalence/inequality of the two approaches, we managed to establish a connection between the fourier components of the two approaches. This opens the feasibility of some research topics, discussed in several papers.

Reference [4] examined the group velocity of a pulse, propagating in an absorbing medium. They derived the average

of the time $\langle t\rangle_x$ that describes where the pulse is in time, for a given space point x. They also announced, eighth reference in this paper, that they would publish a second paper, where they were going to treat the average pulse position $\langle x\rangle_t$ for a given time. They, however, did not publish such a paper. We performed this study, which is very very similar to the method discussed in [4]. The result of $\langle t\rangle_x$ contains the fourier components in real-ω approach $D_1(\omega)$. The result of $\langle x\rangle_t$, however, contains the fourier components in the real-k space $D_2(k)$. Since the two approaches have been unable to be connected, they could not compare the velocity from the two approaches. This is the probable reason for not to publish.

Being established the connection, we plan to investigate average pulse position $\langle x\rangle_t$ and compare the results with the $\langle t\rangle_x$ of reference [4]. For a beginning research we observed that, see figure 9, we showed the group velocity in the two approaches are different. Tracking the propagation of the pulse position (v_2) always results in higher average velocity than the tracking of the arrival time (v_1). This is going to be considered in a separate report.

In the band structure calculations for the frequency dependent dielectric materials, the method of k-real (complex-ω) is also used, [5], in order to compare the results with the ω:complex(k:real) method. The parallel behavior is exhibited. However, the direct relationship between the band structures were not derived.

A proper definition of the group velocity in complex indexed medium, whether uniform or not, has not been established yet. Whatever the formula for a group velocity is, it must generate the same results in both approaches. The closer values of the velocities in two approaches, the generated formula of group velocity is closer to reality.

II. MAXWELL EQUATIONS IN ABSORBING MEDIUM

A. Realness of k

In this section we show that the solution of the Maxwell equations in an absorbing medium is the Fourier integral of real k vectors and complex frequency ω.

Maxwell equations are

$$\begin{array}{ll} \nabla\cdot\mathbf{D}=0 & \nabla\cdot\mathbf{B}=0 \\ \nabla\mathbf{E}=-\frac{\partial\mathbf{B}}{\partial t} & \nabla\mathbf{H}=\frac{\partial\mathbf{D}}{\partial t}. \end{array} \tag{5}$$

For auxiliary magnetic field field we assume vacuum permeability $\mathbf{H}=\frac{\mathbf{B}}{\mu_0}$. Displacement field depends on the the electric field as

$$\mathbf{D}(x,t)=\epsilon_0\mathbf{E}(x,t)+\int_{-\infty}^{\infty}\chi(\tau)\mathbf{E}(x,t-\tau)d\tau. \tag{6}$$

The physical interpretation of equation (6) is as follows. Electron, about the atomic or molecular core, response to the applied electric field in a finite time which is less than the frequency of the light. This creates an electric dipole moment oscillating in time and a magnetization at later times . The dipole moment $\mathbf{M}(x,t)$ at time t, generated by the applied electric field $\mathbf{E}(x,t-\tau)$ at time $t-\tau$, superposes with the the electric field $\mathbf{E}(x,t)$ at time t. Absorbtion of the incident $\mathbf{E}$ field is modelled as the interference with the dipole moment of the medium. This shows, even before attempting to solve Maxwell equations, that the attenuation shall be considered in time.

Due to causality, $\chi(\tau)=0$ for $\tau<0$. dielectric function becomes

$$\mathbf{D}(x,t)=\epsilon_0\mathbf{E}(x,t)+\int_{0}^{\infty}\chi(\tau)\mathbf{E}(x,t-\tau)d\tau. \tag{7}$$

Now, lets solve the Maxwell equations (5) more carefully. Using the third and the fourth equations in (5) we obtain the wave equation

$$\nabla^2\mathbf{E}(x,t)=\frac{1}{c^2}\frac{\partial^2\mathbf{E}}{\partial t^2}+\frac{1}{c^2}\int_0^{\infty}\chi(\tau)\frac{\partial^2\mathbf{E}}{\partial t^2}(x,t-\tau)d\tau \tag{8}$$

for the electric field. Since there is no source $\nabla\cdot\mathbf{E}=0$. We reduce our problem to one dimension, assuming normal incidence. We separate the equation into two, by separation of variables $E(x,t)=E_1(x)E_2(t)$, in time and in space

$$-c^2k^2E_2(t)=\frac{d^2E_2(t)}{dt^2}+\int_0^{\infty}\chi(\tau)\frac{d^2E_2}{dt^2}(t-\tau)d\tau \tag{9}$$

$$-k^2E_1(x)=\frac{d^2E_1(x)}{dx^2}. \tag{10}$$

k^2 is the separation constant, which we have equated to the $-\frac{1}{E_1(x)}\frac{\partial^2E_1(x)}{\partial x^2}$. The solution of space equation (10) is straight forward $E_2(x)=A_2cos(kx)+B_2sin(kx)$ with $E_2(x)$ real.

On the time equation (9) we apparently see that k^2 must be real, since both $\chi(t)$ and $E_2(t)$ are real. Note that the condition for $E(x,t)=E_1(x)E_2(t)$ to be real is both $E_1(x)$ and $E_2(t)$ are to be real. After fixing(choosing) a k value, due to equation (10), we must solve equation (9) for this k value.

To be able to determine $E_2(t;k)$, we Fourier expand the time function of electric field and the dielectric susceptibility as

$$E_2(t)=\textstyle\int_{-\infty}^{\infty}E_2(\omega)e^{-i\omega t}d\omega \quad , \tag{11}$$

$$\chi(\tau)=\textstyle\int_{-\infty}^{\infty}\chi(\omega)e^{-i\omega\tau}d\omega \tag{12}$$

with $E_2(-\omega)=E_2^*(\omega)$ and $\chi(-\omega)=\chi^*(\omega)$. Putting (12) in (9) we determine that $E_2(\omega;k)=0$ for all ω, except for the $\bar{\omega}$ with $\bar{\omega}^2(1+\chi(\bar{\omega}))=c^2k^2$. This equation has two solutions $\bar{\omega}_{1,2}=\pm|\bar{\omega}|$, since $\chi(\omega)$ is symmetric function. (This is also valid for complex ω case when $\omega_R\to-\omega_R$ and $\omega_I\to\omega_I$.)

Then solution, for a fixed k value, is $E_2(t;k)=C_2e^{i|\omega(k)|t}+D_2e^{-i|\omega(k)|t}$. C_2 and D_2 are totally unconnected, except that $E(x,t)$ must be real.

Note that, the form of this solution $E_2(t;k)$ is independent of the solution we chose for $E_1(x)$.

If we use $E_1(x)=cos(kx)$ or $E_1(x)=sin(kx)$, the time solution would be $E_2(t;k)=\mathrm{Re}\{C_2\}cos(\omega(k)t)+\mathrm{Im}\{C_2\}sin(\omega(k)t)$. The solution equivalently can be written in the form

$$\begin{aligned} E_1(x)E_2(t)=e^{ikx}(C_2e^{i|\omega(k)|t}+D_2e^{-i|\omega(k)|t}) \\ +e^{-ikx}(C_2^*e^{-i|\omega(k)|t}+D_2^*e^{i|\omega(k)|t}). \end{aligned} \tag{13}$$

The most general solution, which may contain any k, can be written as

$$E_b(x,t) = \int_{-\infty}^{\infty} dk e^{ikx} \Big(\quad C_2(k) e^{i\omega(k)t} + D_2(k) e^{-i\omega(k)t} \quad \Big), \quad (14)$$

not as

$$E_a(x,t) = \int_{-\infty}^{\infty} d\omega e^{-i\omega t} \Big(\quad C_1(\omega) e^{-ik(\omega)t} + D_1(\omega) e^{ik(\omega)t} \quad \Big). \quad (15)$$

For real $\chi(\omega)$ functions (14) and (15) are equivalent. They are only scaled versions of each other. When $\chi(\omega)$ is complex, however, for a given incident pulse the transmitted pulse(so reflected) may differ in two approaches.

B. Index $n(k)$ and real-k integration

Since ω and k are dependent on each other via $\omega n(\omega) = ck$, we may write equations (14) and (15) as

$$E_b(x,t) = \int_{-\infty}^{\infty} dk e^{ikx} \Big(\quad C_2(k) e^{ickt/n(k)t} + D_2(k) e^{-ickt/n(k)} \quad \Big), \quad (16)$$

$$E_a(x,t) = \int_{-\infty}^{\infty} d\omega e^{-i\omega t} \Big(\quad C_1(\omega) e^{-i\omega n(\omega)x/c} + D_1(\omega) e^{i\omega n(\omega)x/c} \quad \Big). \quad (17)$$

For real $\epsilon(\omega) = n^2(\omega)$, $n(k)$ and $n(\omega)$ are the same within only a transform of the arguments $k \rightarrow \omega n(\omega)/c$. When $\epsilon(\omega)$ is complex, however, $n(k)$ and $n(\omega)$ differs functionally. Moreover, $n(k)$ can not be determined analytically due to the nonlinearity in $n(\omega)$.

When k is constrained to be real, we find index $n(\omega)$ as follows. Equation $n(\omega)\omega = ck$ is now separated into two equations

$$\omega_R n_I + \omega_I n_R = 0 \qquad \text{and} \qquad \omega_R n_R + \omega_I n_I = ck \quad . \quad (18)$$

Since $n_R(\omega)$ and $n_I(\omega)$ are given functions of ω, ω_R and ω_I are solved computationally for a given value of real k. Then, these ω_R and ω_I values are substituted in $n(\omega_R + i\omega_I)$ in order to determine the index value for the real k value, $n(k) = n_R(k) + in_I(k)$.

In figure 1a we plotted the real and imaginary parts of index with respect to real k. And in figure 1b we depicted the corresponding $\omega_R(k)$ and $\omega_I(k)$ values for the real parameter space $k = -2 \ldots 2$. We observe similar properties for $n(k)$, $n_R(-k) = n_R(k)$ and $n_I(-k) = -n_I(k)$, as it is for $n(\omega)$. A zoomed version of $n(k)$ is plotted in figure 2, that is compared with $n(\omega)$. We see that $n(k)$ and $n(\omega)$ are almost the same except that $n(k)$ is little bit greater at both n_R and n_I peaks.

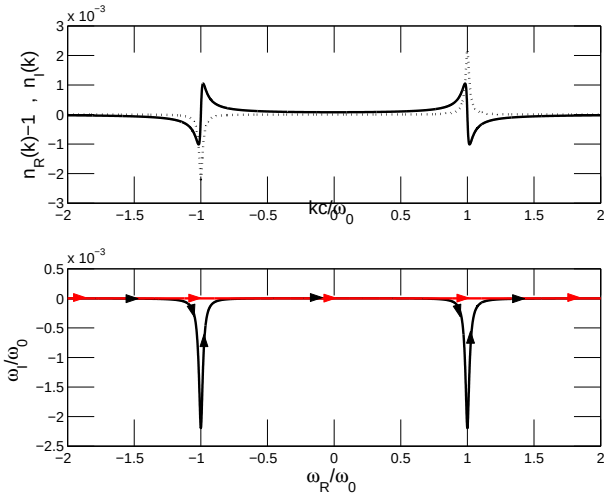

Fig. 1. (a) Complex index as a function of real-k. (b) Corresponding complex frequency $\omega(k) = \omega_R(k) + i\omega_I(k)$ values. This is the real-k integration path $\int_C d\omega$, represented in the complex-ω plane. Red line is the real-ω integration path.

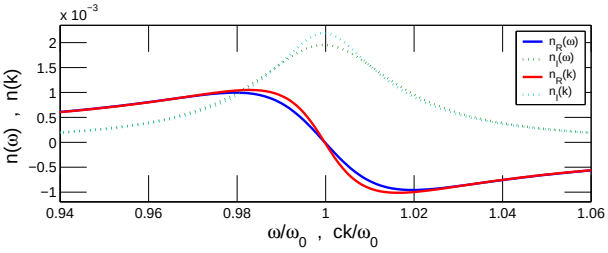

Fig. 2. Complex index for real-ω values $n(\omega)$ and for real-k values. $n(k)$ also exhibits lorentzian type behavior, although analytically not achievable.

C. Integration path in the complex ω plane:

In order to be able to compare functions (16) and (17), we write (14) as

$$\int_C d\omega \left(\frac{dk}{d\omega}\right) e^{i\omega n(\omega)x/c} \Big(\quad C_2\left(\frac{\omega n(\omega)}{c}\right) e^{-i\omega t} + D_2\left(\frac{\omega n(\omega)}{c}\right) e^{i\omega t} \quad \Big) \quad (19)$$

Integration is in the complex ω plane, on the line of constraint k is real. The curve is given in figure 1b with black line. Black arrows indicate the direction of integration, whose limits approaches the real ω axis. The integration with real ω in 17 is drawn with a red line, which is on the real axis. The direction of real ω integration is also indicated with red arrows.

In the next sections we determine the coefficients $D_1(\omega)$, $D_2(k) \equiv D_2\left(\frac{n(\omega)\omega}{c}\right)$ and investigate the difference of functions $E_a(x,t)$ (real ω) and $E_b(x,t)$ (real k).

III. Pulse transmission through an Absorbing Medium

In this section we investigate the pulse transmission through an absorbing medium in 1D. We solve the boundary match problem for the two approaches expressed by electric fields (15) for real ω and (16) for real k.

$n=1$	$n(\omega)=n_R(\omega)+in_I(\omega)$
$E_L(x,t)=$ $\int_{-\infty}^{\infty}d\omega A_1(\omega)e^{i(kx-\omega t)}$ $+\int_{-\infty}^{\infty}d\omega B_1(\omega)e^{i(kx+\omega t)}$	$E_R(x,t)=$ $\int_{-\infty}^{\infty}d\omega D_1(\omega)e^{i(k_1(\omega)x-\omega t)}$
$k=\omega/c$	$k_1=\omega n(\omega)/c$

Fig. 3. The pulse $A(\omega)$, travelling to right, is incident on the plane interface from the air $n=1$. There exist a reflected wave $B_1(\omega)$ on the LHS. On the RHS there is only right travelling wave with frequency components $D_1(\omega)$. The solution on the RHS is considered in real-ω approach.

$n=1$	n=const.
$E_L(x,t)=$ $\int_{-\infty}^{\infty}dkA_2(k)e^{i(kx-\omega t)}$ $+\int_{-\infty}^{\infty}dkB_2(k)e^{i(kx+\omega t)}$	$E_R(x,t)=$ $\int_{-\infty}^{\infty}dkD_2(k)e^{i(kx-\omega_1 t)}$
$\omega=ck$	$\omega_1=ck/n$

Fig. 4. Real-k approach for the constant dielectric. Two approaches are equivalent for real $n(\omega)$.

In subsection III-A we determine the fourier coefficients for real ω case, which we use them to determine $E_a(x,t)$ in the absorbing medium.

In subsection III-B we determine the fourier coefficients for real k case, which we use them to express $E_b(x,t)$. However, we perform this approach in two steps.First for constant dielectric ϵ case, in order to show the equivalence between the two approaches for real $n(\omega)$ case (part III-B1). Second for complex index $n(\omega)$, where two approaches depart from each other (part III-B2).

A. Real ω Approach

We assume a plane interface, see figure 3 , between air $n=1$ and an absorbing medium of complex dielectric $n(\omega)=n_R(\omega)+in_I(\omega)$. Since the incident wave approach from the left(L), there is no left travelling wave on the RHS.

We apply the boundary conditions(BC) $E_{aL}(0,t)=E_{aR}(0,t)$ and $\frac{\partial E_{aL}}{\partial x}(0,t)=\frac{\partial E_{aR}}{\partial x}(0,t)$ to obtain the equations at $x=0$ as

$$\int_{-\infty}^{\infty}d\omega A_1(\omega)e^{-i\omega t}+\int_{-\infty}^{\infty}d\omega B_1(\omega)e^{i\omega t}=\int_{-\infty}^{\infty}d\omega D_1(\omega)e^{-i\omega t} \quad (20)$$

$$\int_{-\infty}^{\infty}d\omega\omega A_1(\omega)e^{-i\omega t}-\int_{-\infty}^{\infty}d\omega\omega B_1(\omega)e^{i\omega t}=\int_{-\infty}^{\infty}d\omega\omega D_1(\omega)e^{-i\omega t} \quad (21)$$

We use the sufficient condition that the integrands are equal for each frequency ω component. Then, fourier components are given by

$$B_1(\omega)=\frac{1-n(\omega)}{1+n(\omega)}A_1(\omega),$$
$$D_1(\omega)=\frac{2}{1+n(\omega)}A_1(\omega). \quad (22)$$

The behavior of the transmitted wave in space and time, is then, given by

$$E_{aR}(x,t)=\int_{-\infty}^{\infty}d\omega\frac{2}{1+n(\omega)}e^{i(n(\omega)\omega x/c-\omega t)} \quad , \quad (23)$$

where each frequency component decay in space with exponential $e^{-n_I(\omega)\omega x/c}$. However the physical intuition (in addition to mathematics) tells that each frequency component must decay in time. This is easily seen by considering an oscillating dipole, which has no interaction with the neighboring dipoles. Since absorption is a local interference effect, the solution must decay in time for a fixed position. One may also tell that equation (23) is only a representation and the decay in time is transferred to the an effective decay in space. We will see in the next section, however, that real k solution differs from (23).

B. Real k Approach

1) Constant Dielectric Case: ϵ : In this part we introduce the real k approach and we show the equivalence (and indicate the reasons of equivalence) between the two approaches when index n is real, see figure 4.

When dielectric response is constant and real, the dispersion $ck=n\omega$ relation comes out only as a scaling transformation between ω and k.

Applying the same BCs, $E_{bL}(0,t)=E_{bR}(0,t)$ and $\frac{\partial E_{bL}}{\partial x}(0,t)=E_{bL}(0,t)=E_{bR}(0,t)$ and $\frac{\partial E_{bR}}{\partial x}(0,t)$, we obtain the integral equations

$$\int_{-\infty}^{\infty}dkA_2(k)e^{-ikct}+\int_{-\infty}^{\infty}dkB_2(k)e^{ikct}=\int_{-\infty}^{\infty}dkD_2(k)e^{-i\frac{k}{n}ct}, \quad (24)$$

$$\int_{-\infty}^{\infty}dkkA_2(k)e^{-ikct}-\int_{-\infty}^{\infty}dkkB_2(k)e^{ikct} \quad (25)$$
$$=\int_{-\infty}^{\infty}dk\frac{k}{n}D_2(k)e^{-i\frac{k}{n}ct} \quad (26)$$

For only mathematical reasons we may define frequency transformations $\omega=ck$ on the LHS and $\omega_1=\frac{ck}{n}$ on the RHS. Equations transform to

$$\frac{1}{c}\int_{-\infty}^{\infty}d\omega A_2(\quad\frac{\omega}{c}\quad)e^{-i\omega t}+\frac{1}{c}\int_{-\infty}^{\infty}d\omega B_2(k)e^{i\omega t}=\frac{n}{c}\int_{-\infty}^{\infty}d\omega_1 D_2(\frac{n\omega_1}{c})e^{-i\omega_1 t}, \quad (27)$$

$$\frac{1}{c^2}\int_{-\infty}^{\infty}d\omega\,\omega A_2(\frac{\omega}{c})e^{-i\omega t}-\frac{1}{c^2}\int_{-\infty}^{\infty}d\omega\omega B_2(k)e^{i\omega t}=\frac{n^2}{c^2}\int_{-\infty}^{\infty}d\omega_1\omega_1 D_2(\frac{n\omega_1}{c})e^{-i\omega_1 t}. \quad (28)$$

Since ω and ω_1 are dummy variables we equate the integrands to obtain the relations

$$A_2\left(\frac{\omega}{c}\right)+B_2\left(-\frac{\omega}{c}\right)=nD_2\left(\frac{n\omega}{c}\right) \quad (29)$$

$n=1$	$n(\omega)\equiv n_R(k)+in_I(k).$
$E_L(x,t)=$ $\int_{-\infty}^{\infty}dkA_2(k)e^{i(kx-\omega t)}$ $+\int_{-\infty}^{\infty}dkB_2(k)e^{i(kx+\omega t)}$	$E_R(x,t)=$ $\int_{-\infty}^{\infty}dkD_2(k)e^{i(kx-\omega_1 t)}$
$\omega=ck$	$\omega_1=ck/n(k)$

Fig. 5. Same configuration of 3, but this time problem is treated with the real-k approach: RHS is expressed as the sum over real-k plane waves of fourier coefficients $D_2(k)$.

$$\omega A_2\left(\frac{\omega}{c}\right)-\omega B_2\left(-\frac{\omega}{c}\right)=n^2\omega D_2\left(\frac{n\omega}{c}\right) \tag{30}$$

between the fourier components. In 30 ω cancels. However, we kept ω in order to remind the reader that $\omega=ck$ on the LHS, but it is $\omega=\frac{ck}{n}$ on the RHS. Consequently the fourier components are calculated to be

$$\begin{aligned} B_2\left(\frac{\omega}{c}\right)&=\frac{1-n}{1+n}A_2\left(\frac{\omega}{c}\right),\\ D_2\left(\frac{n\omega}{c}\right)&=\frac{2}{n(1+n)}A_2\left(\frac{\omega}{c}\right). \end{aligned} \tag{31}$$

Solution of $D_2(k)$ seems different than real ω result (22). However, if it is put in the form $nD_2\left(\frac{n\omega}{c}\right)=\frac{2}{1+n}A_2\left(\frac{\omega}{c}\right)$, it is seen that

$$\int_{-\infty}^{\infty}dkD_2(\omega)e^{ikx-\frac{k}{n}ct}=\int_{-\infty}^{\infty}d\omega\frac{2}{1+n}e^{i\omega x/c-\omega t}. \tag{32}$$

When n is real the results (31) and (22) are equivalent, in determining $E_a(x,t)\equiv E_b(x,t)=E(x,t)$. However, the usual physical interpretation "Frequency does not change for light changing medium between dielectrics." here transforms to only a mathematical scaling transformation which cannot be performed in the complex $\epsilon(\omega)$ case.

2) Complex (frequency-dependent) Dielectric Case: $\epsilon(\omega)=\epsilon_R(\omega)+i\epsilon_I(\omega)$: In this part we discuss the pulse transmission/propagation into/through an absorbing medium. We extend the real-k approach to frequency dependent complex index, $n(\omega)=n_R(\omega)+in_I(\omega)$. We determine the integral equations connecting the fourier components $A_2(k)$, $B_2(k)$ and and $D_2(k)$. The explicit connection, however, is not straightforward to obtain as it is in the real-ω approach. This is left to section IV.

The solutions on the LHS and RHS, see figure 5, are given by

$$\begin{aligned} E_{bL}(x,t) &= \int_{-\infty}^{\infty}dkA_2(k)e^{i(kx-kct)}\\ &\quad+\int_{-\infty}^{\infty}dkB_2(k)e^{i(kx+kct)} \end{aligned} \tag{33}$$

$$E_{bR}(x,t)=\int_{-\infty}^{\infty}dkD_2(k)e^{i\left(kx-\frac{k}{n(k)}ct\right)}\quad. \tag{34}$$

Applying the BC.s $E_{bL}(0,t)=E_{bR}(0,t)$ and $\frac{\partial E_{bL}}{\partial x}(0,t)=\frac{\partial E_{bR}}{\partial x}(0,t)$, as usual, we obtain the integral equations

$$\begin{aligned} \int_{-\infty}^{\infty}dkA_2(k)e^{-ikct} &+ \int_{-\infty}^{\infty}dkB_2(k)e^{ikct}\\ &=\int_{-\infty}^{\infty}dkD_2(k)e^{-i\frac{k}{n(k)}ct}, \end{aligned} \tag{35}$$

$$\begin{aligned} \int_{-\infty}^{\infty}dkkA_2(k)e^{-ikct} &+ \int_{-\infty}^{\infty}dkkB_2(k)e^{ikct}\\ &=\int_{-\infty}^{\infty}dkkD_2(k)e^{-i\frac{k}{n(k)}ct} \end{aligned} \tag{36}$$

This time, however, the fourier components $A_2(k)$ and $B_2(k)$ cannot be connected to $D_2(k)$ easily. This is because we cannot equate the integrands directly, as it is in real-ω approach III-A, or with a scaling transformation, as it is in constant index case III-B1.

One may try to perform the transformation $\omega=ck$ an the LHS and $\omega_2=\frac{ck}{n(k)}$ on the RHS. This time, however, the integral on the RHS transform to a line integration over the complex ω_2 plane as is mentioned in subsection II-B. So, integrands cannot be equalized.

C. The Connection between Fourier Components $D_2(k)$ and $D_1(\omega)$

The incoming pulses are common in both approaches. So that we equate

$$\int_{-\infty}^{\infty}dkA_2(k)e^{i(kx-ckt)}=\int_{-\infty}^{\infty}d\omega A_1(\omega)e^{i(\omega x/c-\omega t)} \tag{37}$$

in order to obtain the relation $\frac{1}{c}A_2(k)=A_1(\omega)$.

Before solving equations (35) and (36) for $D_2(k)$ explicitly, it is not possible to obtain $B_2(k)$ in terms of $A_2(k)$. Without any proof, however, we take

$$B_2(k)=\frac{1-n(k)}{1+n(k)}A_2(k)\quad. \tag{38}$$

This is because we aim to show that the resultant electric fields $E_{aR}(x,t)$ and E_{bR} are different in the absorbing medium. Equation (38) corresponds to taking fourier coefficients equal on the LHS.

When the fourier components on the LHS are the same, functional behavior of $E_{aL}(x,t)$ and $E_{bL}(x,t)$ also match due to scaling transformation $\omega=ck$. Then, the integrals of fourier coefficients on the RHS are also equal

$$\int_{-\infty}^{\infty}dkD_2(k)e^{-i\frac{k}{n(k)}ct}=\int_{-\infty}^{\infty}d\omega D_1(\omega)e^{-i\omega t}. \tag{39}$$

Due to the complexity of the transformation $\omega_2=\frac{ck}{n(k)}$, integrands are not able to be equalized. Furthermore, due to the line integration over the complex ω_2 plane, the presence of equation

$$\begin{aligned} \int_C d\omega\left(\frac{dk}{d\omega}\right)\quad D_2\quad\left(\frac{\omega n(\omega)}{c}\right)e^{-i\omega t}\\ =\int_{-\infty}^{\infty}d\bar{\omega}D_1(\bar{\omega})e^{-i\bar{\omega}t} \end{aligned} \tag{40}$$

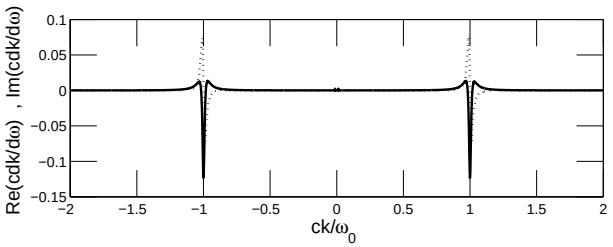

Fig. 6. The behavior of $\frac{dk}{d\omega}$ for real-k case. The real part is symmetric, the imaginary part is anti-symmetric.

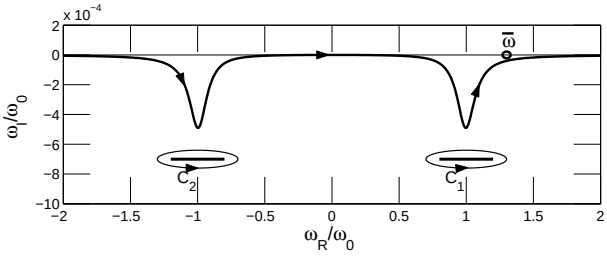

Fig. 7. Real-k integration path, $\int_c d\omega$, in the complex-ω plane.The contours $C_{1,2}$ are the branch cuts of lorentzian $n(\omega)$. There exists no pone nor branch cut of $D_2\left(\frac{n(\omega)\omega}{c}\right)$ in between the curve C and the real-ω axis. The $\bar{\omega}$ is the single pole of equation (47) .

originating from equation (39), *does not imply* the equality

$$\int_C d\omega \left(\frac{dk}{d\omega}\right) \quad D_2 \quad \left(\frac{\omega n(\omega)}{c}\right) e^{i(k(\omega)x-\omega t)} = \int_{-\infty}^{\infty} d\bar{\omega} D_1(\bar{\omega}) e^{i(k(\bar{\omega})x-\bar{\omega}t)}, \quad (41)$$

in general. This is because of the possibility of including any pole or branch cut of $D_2\left(\frac{n(\omega)\omega}{c}\right)$. The bar symbol refers to the reality of frequency.

IV. Difference Between Two Approaches

In the previous section we obtained a direct connection between he fourier components of real-ω approach $D_1(\omega)$ and the ones for the real-k approach $D_2(k)$, at equation (40). In this section we aim to show that this connection leads to different functions for the transmitted pulses $E_{aR}(x,t)$ and $E_{bR}(x,t)$, in the absorbing medium.

We assume that $D_2\left(\frac{n(\omega)\omega}{c}\right)$ converges to zero at all infinities, as $|\omega| \to \infty$. WE make this assumption to be able to use the contour integral formalism; that integration over infinite circles does not contribute.

If ω, on the LHS of equation (40) were real we could use the Dirac delta function formula $\int_{-\infty}^{\infty} e^{-(\omega-\bar{\omega})t} dt = \delta(\omega-\bar{\omega})$ in order to connect $\left(\frac{dk}{d\omega}\right) D_2\left(\frac{n(\omega)\omega}{c}\right)$ to $D_1(\omega)$. The existence of imaginary part of ω, however, makes the time integral divergent. Above, bar symbol $\bar{\omega}$ implies the reality of the variable.

In order to overcome this difficulty we integrate for a finite time, $t = T \ldots T$, after then we take the limit $T \to \infty$. The fourier component of the real-ω approach is given in terms o the real-k approach as

$$2\pi D_1(\bar{\omega}) = \lim_{T\to\infty} \int_C \quad d\omega \quad \left(\frac{dk}{d\omega}\right) D_2\left(\frac{n(\omega)\omega}{c}\right) \times \int_{t=-T}^{T} dt e^{-i(\omega-\bar{\omega})t}, \quad (42)$$

which transforms to

$$2\pi D_1(\bar{\omega}) = \lim_{T\to\infty} \int_C \quad d\omega \quad \left(\frac{dk}{d\omega}\right) D_2\left(\frac{n(\omega)\omega}{c}\right) \times \frac{e^{i(\omega-\bar{\omega})T} - e^{-i(\omega-\bar{\omega})T}}{i(\omega-\bar{\omega})} \quad (43)$$

when the time integration is carried out.

In equation (43) we obtained $D_1(\bar{\omega})$ in terms of $D_2\left(\frac{n(\omega)\omega}{c}\right)$. So, our strategy becomes to place (43) into the solution for the real-ω approach

$$E_{aR}(x,t) = \int_{-\infty}^{\infty} d\bar{\omega} D_1(\bar{\omega}) e^{i(k(\bar{\omega})x-\bar{\omega}t)} \quad (44)$$

to be able to compare $E_{aR}(x,t)$ with the real-k approach solution

$$E_{bR}(x,t) = \int_C d\omega \left(\frac{dk}{d\omega}\right) D_2\left(\frac{n(\omega)\omega}{c}\right) e^{i(k(\omega)x-\omega t)} \quad (45)$$

where integration path C is depicted in figure 1 that is not closed. Equation (45) originates from equation (34).

A. $D_2\left(\frac{n(\omega)\omega}{c}\right)$ has no pole , no branch cut

If $D_2\left(\frac{n(\omega)\omega}{c}\right)$ does not have any pole nor branch cut, see figure 7, integrand in equation (43) has pole only at $\omega = \bar{\omega}$ and branch cut below the real-k contour due to $\left(\frac{dk}{d\omega}\right)$. The $\omega = \bar{\omega}$ pole contributes if real-k contour is closed up for $e^{i(\omega-\bar{\omega})T}$ term and branch cuts contribute if if real-k contour is closed down for $e^{-i(\omega-\bar{\omega})T}$ term. We obtain the relation

$$D_1(\bar{\omega}) = \left(\frac{dk}{d\omega}\right)_{\omega=\bar{\omega}} D_2\left(\frac{n(\bar{\omega})\bar{\omega}}{c}\right) - \lim_{T\to\infty} \sum_{1,2} \oint_{C_{1,2}} d\omega \left(\frac{dk}{d\omega}\right) D_2\left(\frac{n(\omega)\omega}{c}\right) \frac{e^{-i(\omega-\bar{\omega})T}}{2\pi i(\omega-\bar{\omega})}. \quad (46)$$

When we put (46) into (44), electric field for the real-ω approach becomes

$$E_{aR}(x,t) = \int_{-\infty}^{\infty} d\bar{\omega} \left(\frac{dk}{d\omega}\right)_{\omega=\bar{\omega}} D_2\left(\frac{n(\bar{\omega})\bar{\omega}}{c}\right) e^{i(k(\bar{\omega})x-\bar{\omega}t)} - \lim_{T\to\infty} \sum_{1,2} \oint_{C_{1,2}} d\omega \left(\frac{dk}{d\omega}\right) D_2\left(\frac{n(\omega)\omega}{c}\right) \times \times \frac{e^{-i\omega T}}{2\pi i} \int_{-\infty}^{\infty} d\bar{\omega} \frac{e^{i\bar{\omega}T}}{(\omega-\bar{\omega})}. \quad (47)$$

The last integral of the last term of (47) is evaluated by closing the contour up. Defined by $C_{1,2}$ contours, ω is always below the real-ω line. So that, the second term in (47) is zero. Then, electric field for the real-ω approach comes out to be

$$E_{aR}(x,t) = \int_{-\infty}^{\infty} d\bar{\omega} \left(\frac{dk}{d\omega}\right)_{\bar{\omega}} D_2\left(\frac{n(\bar{\omega})\bar{\omega}}{c}\right) e^{i(k(\bar{\omega})x-\bar{\omega}t)} \quad (48)$$

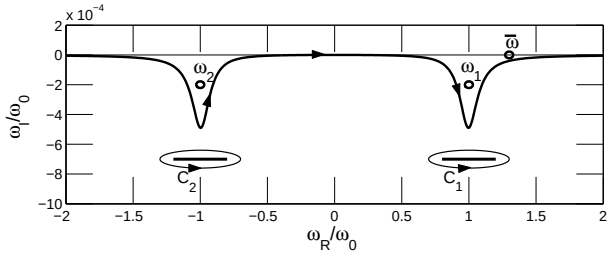

Fig. 8. Real-k integration path, $\int_c d\omega$, in the complex-ω plane. We assume that $D_2\left(\frac{n(\omega)\omega}{c}\right)$ has two symmetric poles at $\omega_1 = \omega_{1R} - i\omega_{1I}$ and $\omega_1 = -\omega_{1R} - i\omega_{1I}$. Equation (51) has three poles at $\omega_{1,2}$ and $\bar{\omega}$.

which is equal to the real-k approach one

$$E_{bR}(x,t) = \int_C d\omega \left(\frac{dk}{d\omega}\right) D_2\left(\frac{n(\omega)\omega}{c}\right) e^{i(k(\omega)x-\omega t)} \quad , \tag{49}$$

because there is no pole nor branch cut of $D_2\left(\frac{n(\omega)\omega}{c}\right)$ in between the integration paths of (48) and (49). In this case both approaches give the same result.

B. $D_2\left(\frac{n(\omega)\omega}{c}\right)$ has pole in between the integration lines

We assume, in difference to the previous case IV-A, that $\left(\frac{dk}{d\omega}\right) D_2\left(\frac{n(\omega)\omega}{c}\right)$ has pole between the two integration lines, see figure 8. If it has a pole at $\omega_1 = \omega_{1R} - i\omega_{1I}$, due to the symmetry property, there must be another pole at $\omega_2 = -\omega_{1R} - i\omega_{1I}$. Then we may express $\left(\frac{dk}{d\omega}\right) D_2\left(\frac{n(\omega)\omega}{c}\right)$ as

$$\left(\frac{dk}{d\omega}\right) \quad D_2 \quad \left(\frac{n(\omega)\omega}{c}\right) = \frac{F(\omega)}{[\omega - (\omega_{1R} - i\omega_{1I})][\omega - (-\omega_{1R} - i\omega_{1I})]} \tag{50}$$

where $F(\omega)$ has the symmetry as $\omega_R \to -\omega_R$. Note that ω_I has same symmetry as $\omega_R \to -\omega_R$.

Closing the contours up, for $e^{i(\omega-\bar{\omega})T}$, 3 poles contribute to $D_1(\omega)$ in (43). Closing the contour down, for $e^{-i(\omega-\bar{\omega})T}$ term, only branch cuts due to $\left(\frac{dk}{d\omega}\right)$ contribute. We obtain

$$\begin{aligned} D_1(\bar{\omega}) &= \left(\frac{dk}{d\omega}\right)_{\bar{\omega}} D_2\left(\frac{n(\bar{\omega})\bar{\omega}}{c}\right) \\ &+ 2\pi i \frac{F(\omega_{1R} - i\omega_{1I})}{2\omega_{1R}} \frac{e^{i(\omega_{1R}-\bar{\omega})T} e^{\omega_{1I}T}}{2\pi i(\omega_1 - \bar{\omega})} \\ &+ 2\pi i \frac{F(-\omega_{1R} - i\omega_{1I})}{-2\omega_{1R}} \frac{e^{i(-\omega_{1R}-\bar{\omega})T} e^{\omega_{1I}T}}{2\pi i(\omega_2 - \bar{\omega})} \\ &- \lim_{T\to\infty} \sum_{1,2} \oint_{C_{1,2}} d\omega \left(\frac{dk}{d\omega}\right) D_2\left(\frac{n(\omega)\omega}{c}\right) \frac{e^{-i(\omega-\bar{\omega})T}}{2\pi i(\omega - \bar{\omega})} \end{aligned} \tag{51}$$

When this is put into equation (44) the last term gives zero, since $e^{i\bar{\omega}T}$ is closed up of the real-ω axis. Due to the symmetry property $F(\omega_1) = F(\omega_2)$. Fourier component of the real-ω case becomes

$$\begin{aligned} D_1 \quad (\bar{\omega}) &= \left(\frac{dk}{d\omega}\right)_{\bar{\omega}} D_2\left(\frac{n(\bar{\omega})\bar{\omega}}{c}\right) \\ + \quad & \frac{F(\omega_1)}{2\omega_{1R}} e^{\omega_{1I}T} e^{-i\bar{\omega}T} \times \\ & \times \left(\frac{e^{i\omega_{1R}T}}{(\omega_{1R} - i\omega_{1I} - \bar{\omega})} - \frac{e^{-i\omega_{1R}T}}{(-\omega_{1R} - i\omega_{1I} - \bar{\omega})}\right) \end{aligned} \tag{52}$$

We put (52) into (44) to determine the electric field for the real-ω approach as

$$\begin{aligned} E_{aR} \quad (x,t) &= \left(\frac{dk}{d\omega}\right)_{\bar{\omega}} D_2\left(\frac{n(\bar{\omega})\bar{\omega}}{c}\right) e^{i(k(\bar{\omega})x-\bar{\omega}t)} \\ + \quad & \lim_{T\to\infty} \frac{F(\omega_1)}{2\omega_{1R}} e^{\omega_{1I}T} \int_{-\infty}^{\infty} d\bar{\omega} e^{-i\bar{\omega}T} e^{i(k(\bar{\omega})x-\bar{\omega}t)} \\ & \times \left(\frac{e^{i\omega_{1R}T}}{(\omega_{1R} - i\omega_{1I} - \bar{\omega})} - \frac{e^{-i\omega_{1R}T}}{(-\omega_{1R} - i\omega_{1I} - \bar{\omega})}\right) \end{aligned} \tag{53}$$

Since T $to\infty$, due to the $e^{-i\bar{\omega}T}$ term real $\bar{\omega}$ integration is closed down. The contour includes two poles at $\bar{\omega} = \omega_{1R} - i\omega_{1I}$ and $\bar{\omega} = -\omega_{1R} - i\omega_{1I}$ and two branch cut loops $C_{1,2}$. Branch cuts occur due to the $e^{ik(\bar{\omega})}$ term. Each branch cut is marked with two points $\omega_{b1} = \omega_{bR1} - i\omega_{bI}$, $\omega_{b2} = \omega_{bR2} - i\omega_{bI}$ for the contour C_1 and $\omega_{b3} = \omega_{bR3} - i\omega_{bI}$, $\omega_{b4} = \omega_{bR4} - i\omega_{bI}$ for the contour C_2. All have same imaginary part. Electric field becomes

$$\begin{aligned} E_{aR}(x,t) &= \int_{-\infty}^{\infty} d\bar{\omega} \left(\frac{dk}{d\omega}\right)_{\bar{\omega}} D_2\left(\frac{n(\bar{\omega})\bar{\omega}}{c}\right) e^{i(k(\bar{\omega})x-\bar{\omega}t)} \\ &+ \lim_{T\to\infty} \frac{F(\omega_1)}{2\omega_{1R}} \left(e^{ik(\omega_1)x-\omega_1 t} - e^{ik(\omega_2)x-\omega_2 t}\right) \\ &+ \lim_{T\to\infty} \frac{F(\omega_1)}{2\omega_{1R}} e^{\omega_{1I}T} e^{-\omega_{bI}T} \\ &\times \left(\int_{\omega_{bR1}}^{\omega_{bR2}} d\omega_{bR} f(\omega_{bR}) + \int_{\omega_{bR1}}^{\omega_{bR2}} d\omega_{bR} f(\omega_{bR})\right), \end{aligned}$$

where the integrals on the last term are carried over the two sides of the each branch cut line. The last term does not contribute, because $\lim_{T\to\infty} e^{\omega_{1I}T} e^{-\omega_{bI}T} = 0$ since $|\omega_{bI}| > |\omega_{1I}|$.

Then the electric field for the real-ω approach (54) is the same with the real-k approach

$$E_{bR}(x,t) = \int_C d\omega \left(\frac{dk}{d\omega}\right) D_2\left(\frac{n(\omega)\omega}{c}\right) e^{i(k(\omega)x-\omega t)}. \tag{55}$$

This is because, the open contour C, joined with the reverse real axis integration, also contains the poles $\omega_{1,2}$.

In this case, too, no difference between the two approaches exists.

V. Average Energy Flow of Optical Pulses in Dispersive Medium

Peatross et. al. [4] analytically derived an expression for the average velocity of a pulse in an absorbing medium. They used the Poynting vector to calculate the average time

$$\langle t \rangle_x = \frac{\int_{-\infty}^{\infty} dt\ t\ S(x,t)}{\int_{-\infty}^{\infty} dt S(x,t)} \tag{56}$$

at which the pulse is on the space point, let it be a detector, x. WE simplified the problem to 1D.

The same problem can be treated in a different point of view: Average spatial position

$$\langle x\rangle_t = \frac{\int_{-\infty}^{\infty} dx\ x\ S(x,t)}{\int_{-\infty}^{\infty} dx S(x,t)} \tag{57}$$

where the pulse is at time t.

One may calculate the pulse velocity referring both to (56) and (57). If Poynting vector average is a good identity to determine the group velocity of a signal, then these two approaches must give similar velocities.

When the index of the medium is complex, (56) is easily treated in the real-ω approach [4] since $S(x,t)$. is easily fourier transformed. Average position (57), however, is easily treated in the real-k approach.

Since the mathematical procedure relating the fourier coefficients $E(x,\omega)$ and $E(k,x)$ has not been studied in a complex indexed medium, however, two group velocity could not be compared.

Being derived the aforementioned connection in the previous subsection III-C, we managed to compare the time arrival velocity (from (56)) and pulse center propagation velocity from (from (57)).

In subsections V-A and V-B we shortly mention the velocity derivation using the real-ω and real-k approaches, respectively. In subsection V-C we compare the two velocities, nothing that they belong to the same pulse.

A. $\langle t\rangle_x$ Real-ω Approach

Since the time average is considered we expend the electric field and magnetic field as

$$\begin{aligned} E(x,t) &= \frac{1}{\sqrt{2\pi}}\int_{-\infty}^{\infty} d\omega E(x,\omega)e^{-i\omega t},\\ H(x,t) &= \frac{1}{\sqrt{2\pi}}\int_{-\infty}^{\infty} d\omega H(x,\omega)e^{-i\omega t}, \end{aligned} \tag{58}$$

where $H(x,\omega) = \frac{k}{\omega}E(x,\omega)$. Then we can write the average Poynting vector(flux) as the frequency component summation

$$\int_{-\infty}^{\infty} dt S(x,t) = \int_{-\infty}^{\infty} d\omega E(x,\omega)H^*(x,\omega), \tag{59}$$

and the average time

$$\int_{-\infty}^{\infty} dt\ t\ S(x,t) = -i\int_{-\infty}^{\infty} d\omega \frac{\partial E(x,\omega)}{\partial\omega}H^*(x,\omega), \tag{60}$$

where we have used the integration by parts, $E(x,\omega = \pm\infty) = 0$, and $t = \frac{1}{-i}\frac{\partial e^{-i\omega t}}{\partial\omega}$.

Time of arrival of a signal from a source at position x_0 to the detector at position x_0 is given by $\Delta t = \langle t\rangle_x - \langle t\rangle_{x_0}$. When we express the temporal dependence explicitly as

$$E(x,\omega) = e^{ik\Delta x}E(x_0,\omega), \tag{61}$$

$$H(x,\omega) = e^{ik\Delta x}H(x_0,\omega) \tag{62}$$

the arrival time becomes

$$\begin{aligned} \Delta t &= -i\times\\ &\times \Big[\frac{e^{-2k_I\Delta x}\int_{-\infty}^{\infty} d\omega\mathcal{F}(\omega;\Delta x,x_0)H^*(x_0,\omega)}{e^{-2k_I\Delta x}\int_{-\infty}^{\infty} d\omega E(x_0,\omega)H^*(x_0,\omega)} \qquad (63)\\ &\quad -\frac{\int_{-\infty}^{\infty} d\omega\frac{\partial E(x_0,\omega)}{\partial\omega}H^*(x_0,\omega)}{\int_{-\infty}^{\infty} d\omega E(x_0,\omega)H^*(x_0,\omega)},\Big] \qquad (64) \end{aligned}$$

where

$$\mathcal{F}(\omega;\Delta x,x_0) = \left\{\left(\frac{\partial k}{\partial\omega}\Delta x\right)E(x_0,\omega) + \frac{\partial E(x_0,\omega)}{\partial\omega}\right\}. \tag{65}$$

This results in a simple arrival time velocity(inverse)

$$\frac{1}{v_1} = \frac{\Delta t}{\Delta x} = \frac{\int_{-\infty}^{\infty} d\omega\frac{\partial k}{\partial\omega}S(x_0,\omega)}{\int_{-\infty}^{\infty} d\omega S(x_0,\omega))}, \tag{66}$$

where complex harmonic Poynting vector is defined as $S(x_0,\omega) = E(x_0,\omega)H^*(x_0,\omega)$. Note that wave-vector k is complex.

B. $\langle x\rangle_t$ Real-k Approach

When the spatial average is considered we expend the electric field and magnetic field as

$$E(x,t) = \frac{1}{\sqrt{2\pi}}\int_{-\infty}^{\infty} dkE(k,t)e^{ikx}, \tag{67}$$

$$H(x,t) = \frac{1}{\sqrt{2\pi}}\int_{-\infty}^{\infty} dkH(x,\omega)e^{ikx}, \tag{68}$$

where $H(k,t) = \frac{k}{\omega}E(k,t)$, again. Then we can write the average Poynting vector(flux) as the frequency component summation

$$\int_{-\infty}^{\infty} dxS(x,t) = \int_{-\infty}^{\infty} dkE(k,t)H^*(k,t), \tag{69}$$

and the average spatial pulse position

$$\int_{-\infty}^{\infty} dx\ x\ S(x,t) = i\int_{-\infty}^{\infty} dk\frac{\partial E(k,t)}{\partial k}H^*(k,t), \tag{70}$$

where we have used the integration by parts, $E(k=\pm\infty,t) = 0$, and $x = \frac{1}{i}\frac{\partial e^{ikx}}{\partial k}$.

The change of the pulse center position from at time t_0 to at time t is given by $\Delta x = \langle x\rangle_t - \langle x\rangle_{t_0}$. When we express the temporal dependence explicitly as

$$E(k,t) = e^{-i\omega\Delta t}E(k,t_0), \tag{71}$$

$$H(k,t) = e^{-i\omega\Delta t}H(k,t_0), \tag{72}$$

we obtain the pulse center propagation velocity

$$v_2 = \frac{\Delta x}{\Delta t} = \frac{\int_{-\infty}^{\infty} dk\frac{\partial\omega}{\partial k}S(k,t_0)}{\int_{-\infty}^{\infty} dkS(k,t0))}. \tag{73}$$

complex Poynting vector is defined as

$$S(k,t_0) = E(k,t_0)H^*(k,t_0). \tag{74}$$

Now, frequency ω is complex.

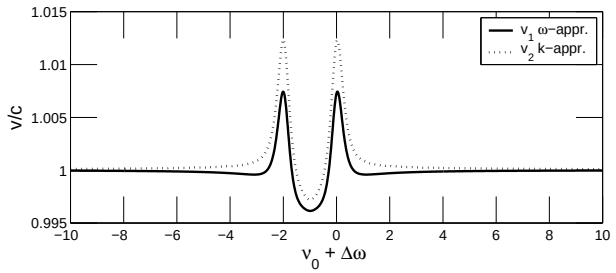

Fig. 9. (solid-line) Group velocity calculated by Poynting vector average $\langle t\rangle_{x_0}$ for fixed position x_0. Treated in real-ω approach. (dotted-line) Group velocity calculated by Poynting vector average $\langle x\rangle_{t_0}$ for fixed time x_0. Treated in real-k approach.

C. Comparison of the Velocities

We assume fourier distributions $D_1(\omega)$ and $D_2(k)$ which does not have any poles nor branch cuts in between the integration paths depicted in figure 1. Then we are able to use the identity (46), $D_1(\bar{\omega}) = \left(\frac{dk}{d\omega}\right)_{\bar{\omega}} D_2\left(\frac{\bar{\omega} n(\bar{\omega})}{c}\right)$. Note that the second term in (46) approaches zero as $T \to \infty$, since all ω on $C_{1,2}$ are complex.

The fourier components are $E(x_0,\omega) \equiv D_1(\omega)$ and $E(k,t_0) \equiv D_2(k)$. Magnetic field components are $H(x_0,\omega) \equiv \frac{k(\omega)}{\omega} D_1(\omega) = n(\omega) D_1(\omega)$ and $E(k,t_0) \equiv \frac{k}{\omega(k)} D_2(k) = n(k) D_2(k)$. Then the first velocity becomes

$$v_1 = \frac{\int_{-\infty}^{\infty} d\bar{\omega} n^*(\bar{\omega}) |D_1(\bar{\omega})|^2}{\int_{-\infty}^{\infty} d\bar{\omega} n^*(\bar{\omega}) \frac{dk}{d\omega}(\bar{\omega}) |D_1(\bar{\omega})|^2} \quad , \tag{75}$$

where $\bar{\omega}$ indicates the reality of the frequency.

Since there is no pole between the integration paths, Fig. 7, second velocity can be written as

$$\begin{aligned} v_2 &= \frac{\int_C d\omega \frac{dk}{d\omega} \frac{d\omega}{dk} n^*(\omega) |D_2(k(\omega))|^2}{\int_C d\omega \frac{d\omega}{dk} n^*(\omega) |D_2(k(\omega))|^2} \\ &= \frac{\int_{-\infty}^{\infty} d\bar{\omega} n^*(\bar{\omega}) |D_2(k(\bar{\omega}))|^2}{\int_{-\infty}^{\infty} d\bar{\omega} \frac{d\omega}{dk}(\bar{\omega}) n^*(\bar{\omega}) |D_2(k(\bar{\omega}))|^2} \quad . \end{aligned} \tag{76}$$

If we use (46) as $D_2(k(\bar{\omega})) = \left(\frac{d\omega}{dk}\right)_{\bar{\omega}} D_1(\bar{\omega})$, we transform v_2 into the form

$$v_2 = \frac{\int_{-\infty}^{\infty} d\bar{\omega} n^*(\bar{\omega}) \left|\frac{d\omega}{dk}(\bar{\omega})\right|^2 |D_1(\bar{\omega})|^2}{\int_{-\infty}^{\infty} d\bar{\omega} \frac{d\omega}{dk}(\bar{\omega}) n^*(\bar{\omega}) \left|\frac{d\omega}{dk}(\bar{\omega})\right|^2 |D_1(\bar{\omega})|^2} \quad . \tag{77}$$

Since v_2, in equation (77), is written in terms of the fourier coefficients of the real-ω approach, we are able to compare the results of the two velocities (75) and (77).

For the frequency spectrum we chose a lorentzian distribution $D_1(\omega) = \frac{1}{[\omega-(\nu_0+\Delta\omega-i\zeta)][\omega-(-\nu_0-\Delta\omega-i\zeta)]}$, whose poles are below the lorentzian index $n(\omega) = \frac{[\omega-(\beta_0-i\rho)]^{1/2}[\omega-(-\beta_0-i\rho)]^{1/2}}{[\omega-(\nu_0-i\rho)]^{1/2}[\omega-(-\nu_0-i\rho)]^{1/2}}$, since $\zeta > \rho$. We used $\rho = \gamma/2$ and $\nu_0^2 = \omega_0^2 + \rho^2$, which are defined in [2].

The numerical results are depicted in figure 9. We observe that real-k approach (77) results in higher velocity everywhere than real-ω approach (75).

Then, the velocity of the center of pulse propagation in spatially is always greater than the average arrival time velocity.

We plan to check the similar velocities for defined as the energy average.

D. Why to treat $\langle t\rangle_x$ and $\langle x\rangle_t$ in different approaches?

In section V-A, while calculating the time average $\langle t\rangle_x$, we used the real-ω approach. In section V-B, while calculating position average $\langle x\rangle_t$, we preferred to use the real-k approach. This parallelism, at first, may seem like that; we performed the calculation of the same quantity in the two approaches and found different results. This is a misunderstanding.

The true story is as follows. After we showed the equivalence of the two approaches, in section IV, we calculated the two different quantities $\langle t\rangle_x$ and $\langle x\rangle_t$. The first is analytically trackable in the real-ω approach, second is in the real-k approach.

As an example we try to treat spatial average $\langle x\rangle_t$ in the real-ω approach, and show the dead-end. Starting from equation (57) we fourier expand the electric fields with real-ω's

$$\begin{aligned} \int_{-\infty}^{\infty} dx\, x\, S(x,t) &= \frac{1}{2\pi} \int_{-\infty}^{\infty} dx \int_{-\infty}^{\infty} d\omega_1 \int_{-\infty}^{\infty} d\omega_2 \times \\ &\times \frac{1}{i} \frac{\partial e^{ik(\omega_1)x}}{\partial k(\omega_1)} e^{-i\omega_1 t} E(\omega_1) e^{ik(\omega_2)x} e^{-i\omega_2 t} \frac{k(\omega_2)}{\omega_2} E(\omega_2), \end{aligned} \tag{78}$$

which can be put in to the form, using similar arguments as in equation (64),

$$\begin{aligned} \Delta x &= \int_{-\infty}^{\infty} dx \int_{-\infty}^{\infty} d\omega_1 \int_{-\infty}^{\infty} d\omega_2 \left(\frac{\partial \omega_1}{\partial k(\omega_1)} \Delta t\right) E(\omega_1) \\ &\times \frac{k(\omega_2)}{\omega_2} E(\omega_2) e^{ik(\omega_1)x} e^{-i\omega_1 t} e^{ik(\omega_2)x} e^{-i\omega_2 t} \ . \end{aligned} \tag{79}$$

This is, however, cannot be simplified further. Because integral

$$\int_{-\infty}^{\infty} dx e^{ik(\omega_1)x} e^{ik(\omega_2)x} \neq 2\pi\delta(k_1 - k_2) \ , \tag{80}$$

since k_1 and k_2 are now complex. Furthermore, this integral diverges. In order to make a progress in (79), one already has to study the mathematics of the previous sections.

ACKNOWLEDGMENT

I acknowledge support from TÜBİTAK-KARİYER Grant No. 112T927 and TÜBİTAK-1001 Grant No. 110T876. I specially thank T. Çetin Akıncı and Ş. Serhat Şeker for their motivational support.

REFERENCES

[1] M.E. Taşgın, Phys. Rev. A **86**, 033833 (2012).
[2] J.D. Jackson, *Classical Electrodynamics*(Wiley, Newyork, 1998), 3rd ed., pp. 336, 348
[3] M. Tanaka, M. Fujiwara, and Hideo Ikegami, Phys. Rev. A, **34**, 4851 (1986)
[4] J. Peatross, S.A. Glasgow, and M. Ware, Phys. Rev. Lett. **84** 2370 (2000)
[5] V. Kuzmiak and A.A. Maradudin, Phys. Rev. B **55**, 7427 (1997).
[6] M. Fleischhauer, C.H. Keitel, M.O. Scully, C. Su, B.T. Ulrich, and S.Y. Zhu, Phys. Rev. A **46**, 1468 (1992).
[7] M.O. Scully and M.S. Zubairy, *Quantum Optics* (Cambridge University Press, Cambridge, 1997).

Mehmet Emre Taşgın received the B.S. degree in physics from Bilkent University, Ankara, Turkey, in 2003 and the Ph.D. degree in physics from Bilkent University, Ankara, Turkey, in 2009. He performed a one year post-doc at Koç University, İstanbul, Turkey, in 2010. He did another one year post-doc in the College of Optics, at University of Arizona, Tucson, AZ, USA, in 2011. Starting from 2012, he is an Asst. Prof. in the Department of Electrical and Electronics Engineering at Kırklareli University, Kırklareli, Turkey. His research interests are quantum optical properties cold atoms, photonic crystals, quantum measurements, spin-squeezing, and electromagnetically induced transparency-like effects in solar cells.